Experimental and Mechanistic Modeling of Fast Pyrolysis of Neat Glucose-Based Carbohydrates. 2. Validation and Evaluation of the Mechanistic Model

ARTICLE *in* INDUSTRIAL & ENGINEERING CHEMISTRY RESEARCH · AUGUST 2014

Impact Factor: 2.59 · DOI: 10.1021/ie502260q

4 AUTHORS, INCLUDING:

Xiaowei Zhou
Northwestern University
12 PUBLICATIONS **67** CITATIONS
SEE PROFILE

Brent H. Shanks
Iowa State University
138 PUBLICATIONS **3,272** CITATIONS
SEE PROFILE

I&EC research
Industrial & Engineering Chemistry Research

Article

pubs.acs.org/IECR

Experimental and Mechanistic Modeling of Fast Pyrolysis of Neat Glucose-Based Carbohydrates. 2. Validation and Evaluation of the Mechanistic Model

Xiaowei Zhou,[†] Michael W. Nolte,[‡] Brent H. Shanks,[‡,§] and Linda J. Broadbelt*[,†]

[†]Department of Chemical and Biological Engineering, Northwestern University, 2145 Sheridan Road, Evanston, Illinois 60208, United States

[‡]Department of Chemical and Biological Engineering, Iowa State University, 2119 Sweeney Hall, Ames, Iowa 50011, United States

[§]Center for Biorenewable Chemicals (CBiRC), Iowa State University, 1140 Biorenewables Research Laboratory Building, Ames, Iowa 50011, United States

Supporting Information

ABSTRACT: A computational framework based on continuous distribution kinetics was constructed to solve the mechanistic model that was developed for fast pyrolysis of glucose-based carbohydrates in the first part of this study [Zhou et al. *Ind. Eng. Chem. Res.* **2014**, 53. DOI 10.1021/ie502259w]. Comparing modeling results with experimental yields from fast pyrolysis over a wide range of reaction conditions validates the model. Agreement between model yields of final pyrolysis products with experimental data of fast pyrolysis of cellulose at temperatures ranging from 400 to 600 °C and maltohexaose, cellobiose, and glucose at 500 °C showed that the mechanistic model was robust and extendable. In comparison to our previous model [Vinu, R.; Broadbelt, L. J. *Energy Environ. Sci.* **2012**, 5, 9808−9826], the mechanistic model presented in this work incorporating new findings from experiments and theoretical calculations showed enhanced performance in capturing experimental yields of major products such as levoglucosan-pyranose, char, H_2O, CO_2, CO, and especially glycolaldehyde and 5-hydroxymethylfurfural. The model was also able to well match the yields of pyrolysis products that our previous model did not include, such as levoglucosan-furanose, methyl glyoxal, and minor products with yields of less than 1 wt % like levoglucosenone, acetone, dihydroxyacetone, and propenal. The mechanistic model showed its versatility in providing insights that were difficult to obtain from experiments, including a time scale of 4−5 s for complete thermoconversion of cellulose at 500 °C. Analysis of the contributions of competing reaction pathways showed that decomposition of cellulosic chains played a more important role in the formation of levoglucosan and glycolaldehyde than in that of other pyrolysis products.

1. INTRODUCTION

Fast pyrolysis, a promising strategy for the production of renewable transportation fuels and chemicals from lignocellulosic biomass, involves a complex network of competing reactions, which result in the formation of bio-oil, non-condensable gaseous species, and solid char.[1,2] Bio-oil is a mixture of anhydro sugars, furan derivatives, and oxygenated aromatic and low molecular weight products (LMWPs). Previously, the successful modeling of fast pyrolysis reactors for biomass conversion was limited to lumped kinetic models, which fail to predict the bio-oil composition.[3−5] Hence, a fundamental understanding of the chemistry and kinetics of biomass pyrolysis is important to evaluate the effects of process parameters like temperature, residence time, and pressure on the composition of bio-oil. Toward this end, in the first part of this study (DOI 10.1021/ie502259w), a unified mechanistic model, which included the decomposition of cellulosic polymer chains and reactions of glucose intermediates along with a range of low molecular weight (LMW) species, was developed for fast pyrolysis of cellulose as well as other glucose-based carbohydrates by integrating up-to-date findings obtained through experiments and quantum chemical calculations.

The primary purpose of this paper is to solve, validate, and evaluate the mechanistic model. A computational framework based on continuous distribution kinetics was constructed to solve the mechanistic model. Validation of the model was performed by comparing model outputs with experimental results obtained from fast pyrolysis of cellulose at 400−600 °C and maltohexaose, cellobiose, and glucose at 500 °C, which were reported inthe first part of this study (DOI 10.1021/ie502259w). Analysis of the net rates of competing reactions was performed. Contributions of different pathways for the formation of levoglucosan and glycolaldehyde and effects of the initial chain length of cellulose on the pyrolysis product distribution are discussed. Insights and information that the model provides lead to a better understanding of fast pyrolysis at the mechanistic level.

2. MODELING FRAMEWORK AND SOLUTION APPROACH

Having specified the mechanism in terms of elementary steps, rate coefficients in terms of the Arrhenius parameters, activation energy (E_a) and frequency factor (A), and species

Received: June 5, 2014
Revised: July 23, 2014
Accepted: July 24, 2014
Published: July 24, 2014

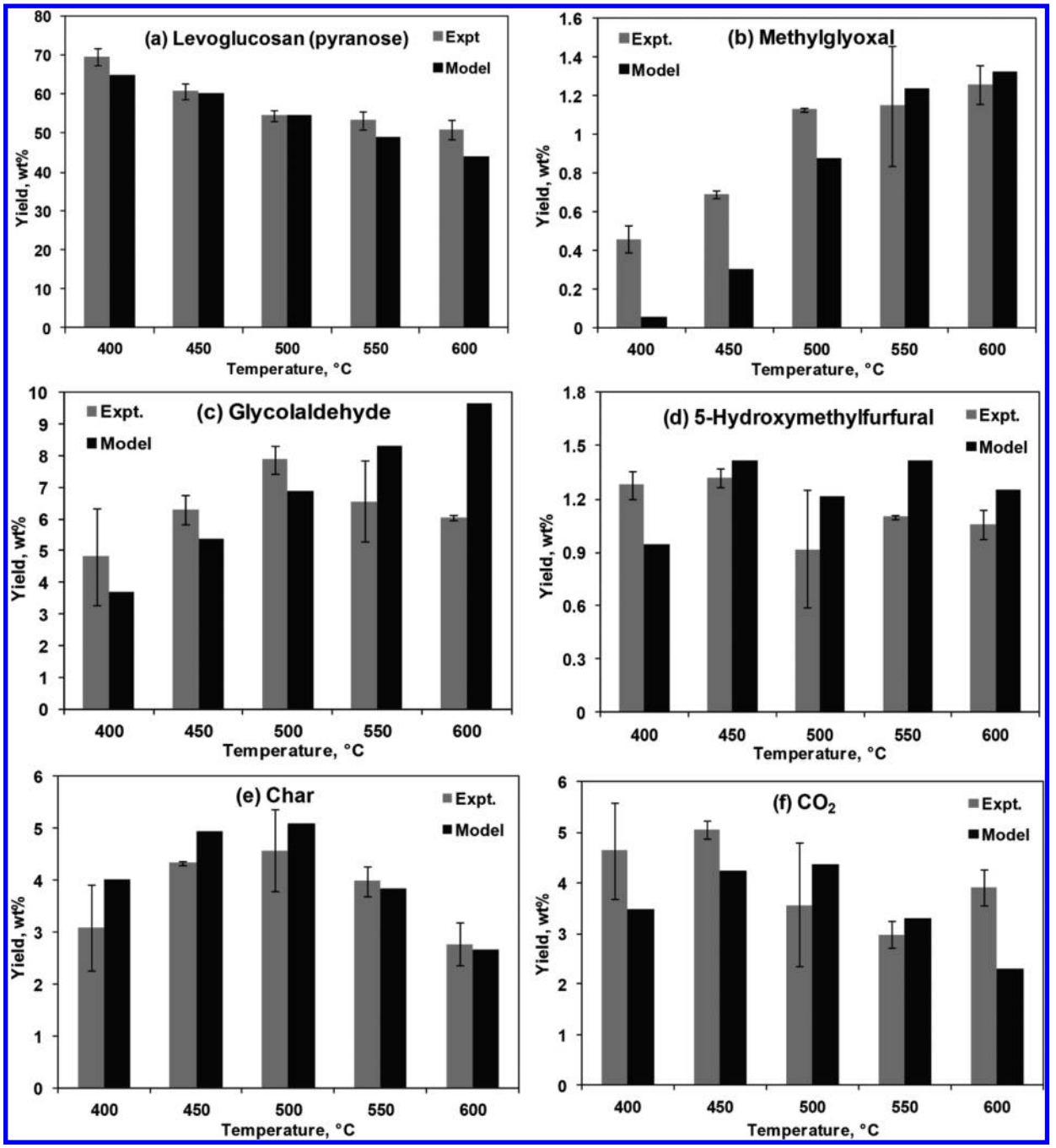

Figure 1. Comparisons between model output and experimental yields of major products obtained from fast pyrolysis of cellulose at different temperatures ranging from 400 to 600 °C. The experimental error bars correspond to the standard deviation of triplicate runs for fast pyrolysis of cellulose.

identity in terms of polymeric chains (end-groups and mid-groups) and LMW species in the first part of the study (DOI 10.1021/ie502259w; reaction mechanism for fast pyrolysis of cellulose is described in Schemes S1−S5 in the Supporting Information), the next step in the modeling framework is to generate rate equations and accompanying approximations to solve the model as well as to evaluate the time evolution of the pyrolysis products. In this model, the initial chain length of the glucose-based carbohydrate(s) and the pyrolysis temperature are model inputs and reaction time is an independent variable. Continuous distribution kinetics was adopted here to describe the rates of decomposition of cellulosic chains. The concentrations of cellulosic polymer chains are modeled as a function of chain length and pyrolysis time, resulting in integro-differential rate equations.[6,7] Moment operations were employed to transform them into ordinary differential equations (ODEs).[6,8,9] On the basis of the mechanism in Schemes S1 and S2 in the Supporting Information, the model includes three different types of reactions of the cellulosic chains, which are (i) unimolecular random cleavage of the chains, (ii) unimolecular unzipping of LMWPs from the chains, and (iii) bimolecular thermohydrolysis. For example, initiation (reaction I in Scheme S1 in the Supporting Information) falls under category i.

dx.doi.org/10.1021/ie502260q | Ind. Eng. Chem. Res. 2014, 53, 13290−13301

$$C(x) \xrightarrow{k_{init}(x)} C_{LVG}(x - x') + C'(x') \quad (1)$$

This reaction involves the cleavage of a glycosidic bond at any random position in the cellulose chain, C, of chain length x, resulting in the formation of a cellulose chain terminated by an LVG end, C_{LVG}, of chain length $x - x'$, and another cellulose chain C' of chain length x'. The rate of this reaction is linearly dependent on chain length, $k_{init}(x) = k_{init}{}^{*}x$.[10] The even distribution of products along all $x' \leq x$ is given by the random stoichiometric kernel, $\Omega_{Rand}(x',x) = 1/x$.[10] The rate equations, after applying moments on the initial population balance equation, are given as follows,

$$\frac{dC^{(m)}}{dt} = -k_{init}C^{(m+1)} \quad (2)$$

$$\frac{dC^{m}_{LVG}}{dt} = \frac{dC'^{(m)}}{dt} = \frac{k_{init}}{m+1}C^{(m+1)} \quad (3)$$

where the moments, $C^{(0)}$, $C^{(1)}$, and $C^{(2)}$ denote molar concentration, mass concentration, and second moment, respectively. Number-average (M_n) and weight-average molecular weight (M_w) of cellulose are given by $C^{(1)}/C^{(0)}$ and $C^{(2)}/C^{(1)}$, respectively. The Saidel−Katz approximation was utilized to close the moments for the third moment, $C^{(3)}$, as shown in eq 4.[7]

$$C^{(3)} = 2\frac{C^{(2)}C^{(2)}}{C^{(1)}} - \frac{C^{(2)}C^{(1)}}{C^{(0)}} \quad (4)$$

The rate equations associated with all the reactions of the cellulosic chains have been described in our previous work.[3] Detailed derivation of these equations can be found elsewhere.[6,7]

All the LMW species were assumed to react according to mass action kinetics with rate laws based on elementary steps and rate coefficients calculated using the Arrhenius equation, viz., $k = A\exp(-E_a/RT)$. Programs were developed using programming languages Perl and C++ to automatically generate the rate equations and the associated algebraic equations (for bond probabilities and third moment of polymer chain distribution), which were solved using DDASAC.[11] A semibatch reactor model that tracks the reduction in volume of the melt phase caused by the vaporization of LMWPs was established, in which various cellulosic chains, C5 and C6 sugars, dehydrated sugars, and char were accounted for in the melt phase, while all other LMWPs were accounted for in the vapor phase. The number-average molecular weight and polydispersity of microcrystalline cellulose, corresponding to the samples utilized in the first part of this study (DOI 10.1021/ie502259w), were estimated to be 135 554 g·mol^{-1} (degree of polymerization, DP = 836) and 2.25, respectively. The initial molecular weight of 991 g·mol^{-1} and the polydispersity of 1.0 were used for maltohexaose. Values of 1540, 1529, and 1420 g·L^{-1} were utilized for the mass densities of glucose, cellobiose, and cellulose/maltohexaose, respectively.

3. RESULTS AND DISCUSSION

To validate the mechanistic model and evaluate its performance, the yields of pyrolysis products captured by the model are compared with experimental results from fast pyrolysis of glucose-based carbohydrates. Details on the operating method and quantification procedure can be found in the first part of this study (DOI 10.1021/ie502259w). Briefly, fast pyrolysis of 200−500 μg of cellulose at temperatures ranging from 400 to 600 °C and maltohexaose, cellobiose and glucose at 500 °C was conducted in a Frontier Laboratories 2020 iS single-shot micropyrolyzer. The pyrolysis products were identified using a mass spectrometery (MS) instrument (Saturn 2000) and quantified using a flame ionization detector (FID). Experimental yields of pyrolysis products and corresponding standard deviation for triplicate pyrolysis runs are given in Tables S1−S4 in the Supporting Information.

3.1. Fast Pyrolysis of Neat Cellulose at Different Temperatures. Figure 1 presents the experimental comparisons for the major products, viz., (a) levoglucosan (pyranose), (b) methyl glyoxal, (c) glycolaldehyde (GA), (d) 5-hydroxymethylfurfural (5-HMF), (e) char, and (f) CO_2 from fast pyrolysis of neat cellulose at 400, 450, 500, 550, and 600 °C. The product yields correspond to ca. over 99 wt % conversion of cellulose. The model gives excellent agreement for the dominant pyrolysis product levoglucosan (pyranose) in terms of the final yields and the overall trend with temperature. Although the yields of methyl glyoxal are underestimated a bit at temperatures of 400 and 450 °C, the model captures the yield trend well at all temperatures. For glycolaldehyde, the model yields match well with the experimental yields over the temperature range of 400−500 °C but are overestimated at higher temperatures of 550 and 600 °C. The precursors of formation of glycolaldehyde (reactions ix, 5, 9, and 61) such as anhydroglucopyranose would be more volatile and more likely to escape the reaction zone and thus no longer be converted into glycolaldehyde at higher temperatures, accounting for the decreasing yield that was observed in the experiments. The overpredicted yields of glycolaldehyde at higher temperatures can be attributed to the model not making a fine enough distinction in the vapor pressure of various compounds as a function of structure and temperature, and efforts to more precisely capture the volatility of all species as a function of structure and reaction conditions represent a significant further advance in the model that is currently in progress. Thus, glycolaldehyde was allowed to form from compounds that were assumed to stay in the melt phase. Because of the incorporation of a new pathway for the formation of 5-HMF from glucose via the fructose intermediate that was recently revealed by Mayes et al.,[12] better performance is shown in terms of matching experimental yields of 5-HMF from fast pyrolysis of cellulose at different temperatures, as compared to our previous model.[3] Even though the char formation step is not fully mechanistic in the model because of the complex structure of char varying with temperature, the model also gave strikingly good agreement with experimental data in terms of the final yields of char and the overall trends at all temperatures. Large errors for experimental yields of char at 400 and 500 °C (Figure 1e) result from char measurements being challenging to reproduce because of difficulty in obtaining char from the reaction vessel and also accurately measuring its low mass (usually <40 μg) after pyrolysis.

The improved performance of the mechanistic model is even better demonstrated by showing how well it predicts the minor products with yields of less than 1 wt % as well as the products that were newly added compared to our previous model. It is important to reiterate that more pyrolysis intermediates and products have been identified and quantified in recent experimental work reported in the literature,[12,13] and one of the major contributions of this work is to incorporate more pyrolysis chemistry involving these compounds, such as

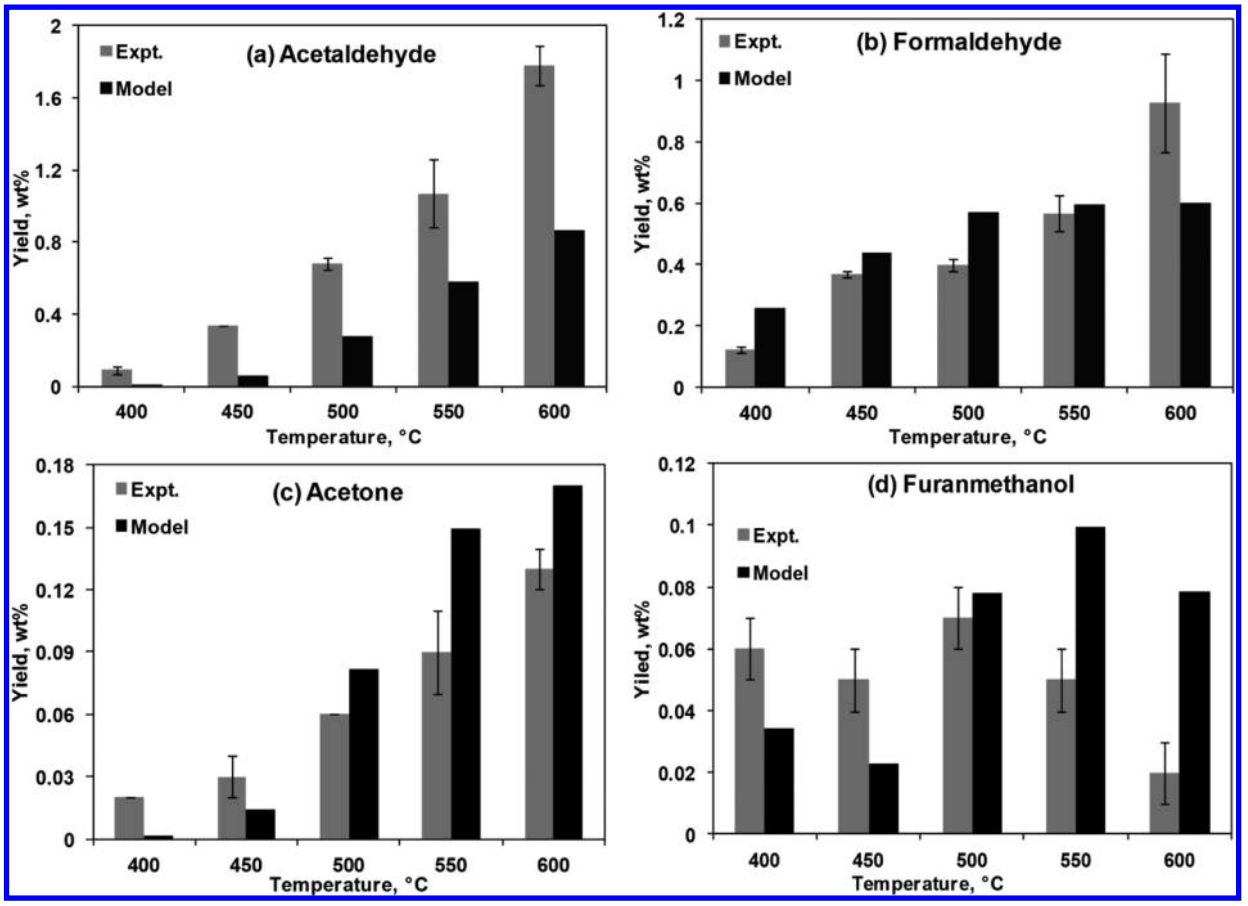

Figure 2. Comparisons between model output and experimental yields of minor products obtained from fast pyrolysis of cellulose at different temperatures ranging from 400 to 600 °C. The experimental error bars correspond to the standard deviation of triplicate runs for fast pyrolysis of cellulose.

levoglucosan (furanose), methylglyoxal, cyclic hydroxyl lactone, acetone, dihydroxyacetone, levoglucosenone, and propenal, into the mechanistic model. The model tracks 67 LMWPs, as compared to 40 LMWPs covered by our previous model. Figure 2 describes four representative comparisons between model output and experimental yields of (a) acetaldehyde, (b) formaldehyde, (c) acetone, and (d) furanmethanol obtained from fast pyrolysis of cellulose at different temperatures. As shown in Figure 2a, although the yields of acetaldehyde are underestimated, the model yields follow the same trend as experimentally observed. The increase in yields of acetaldehyde with elevated pyrolysis temperature is attributed to its formation involving the retro-Diels–Alder reaction of anhydroglucopyranose, which requires a relatively high activation energy of 55 kcal·mol^{-1} and thus is favored at high temperature. The model closely matches the experimental yields of formaldehyde at all temperatures except 600 °C (Figure 2b). The underestimated yield of formaldehyde at 600 °C is likely attributed to the secondary reactions of some LMWPs in the gas phase at the highest temperature, which the model has not included. Noticeably, the model yields and their trends match very well with experimental ones for minor products such as formaldehyde and especially acetone (Figure 2c) which is a product that was newly added and has a yield of less than 0.2 wt %. Similarly, the yield of acetone, which is formed by decarbonylation with an activation energy of 60 kcal·mol^{-1}, also sharply increases with rising temperature. The model gives reasonable agreement for furanmethanol (Figure 2d) that has an even lower yield of less than 0.1 wt %.

Importantly, this model captures experimental yields of various pyrolysis products at different pyrolysis temperatures without the help of a temperature exponent for any elementary reactions, further supporting its improvement compared to our first model. Furthermore, the good agreement between model results and experimental yields over such a wide temperature range testifies to the robustness of the model and also validates that the rate parameters (please see Table S5 in the Supporting Information for activation energies) being utilized for the various reactions quantitatively describe the transformations occurring at fast pyrolysis characterized by high temperature, high heating rate, and high rate of product removal.

3.2. Fast Pyrolysis of Neat Glucose, Cellobiose, and Maltohexaose. The primary advantage of this mechanistic model, which is built based on elementary reactions, is that it is extendable for a wide range of operating conditions. Having demonstrated its capability of closely capturing the yields of various products for cellulose fast pyrolysis over a wide range of temperatures, this section explores the applicability of the model to understand the reaction kinetics and mechanisms of fast pyrolysis of glucose-based carbohydrates like glucose, cellobiose, and maltohexaose that share the same chemistry. Note that kinetic parameters were fitted to match only experimental data from fast pyrolysis of cellulose. Therefore, modeling results for glucose, cellobiose, and maltohexaose are

dx.doi.org/10.1021/ie502260q | Ind. Eng. Chem. Res. 2014, 53, 13290–13301

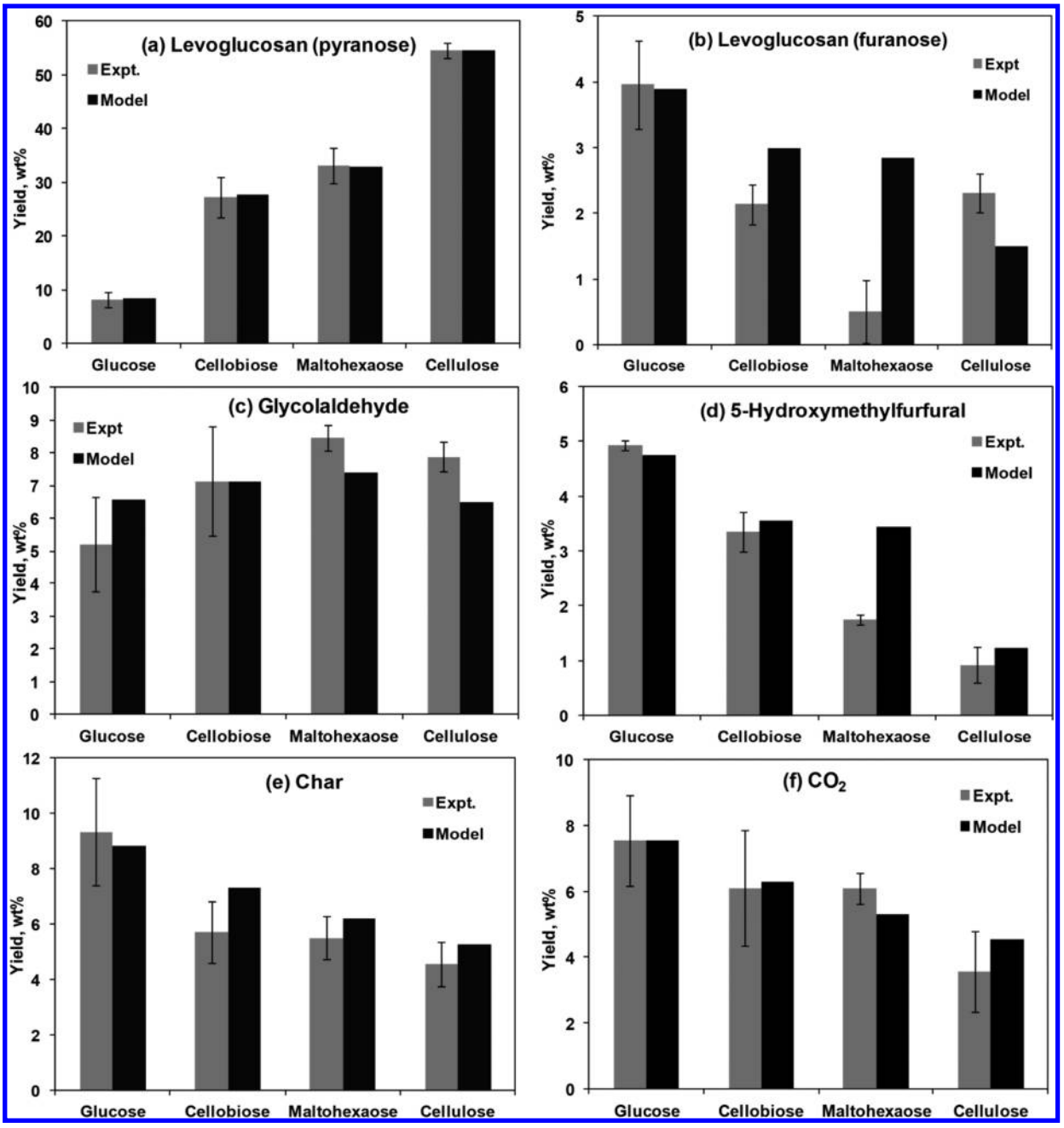

Figure 3. Comparisons between model predictions and experimental yields of major products obtained from fast pyrolysis of glucose-based carbohydrates (glucose, cellobiose, maltohexaose, and cellulose) at 500 °C. The experimental error bars correspond to the standard deviation of triplicate fast pyrolysis runs for each case.

pure predictions and are compared with the experimental data to evaluate the predictive capability of the model.

Figures 3 and 4 show the comparisons of model yields of various products, including major, minor, and newly included products, versus experimental data obtained from fast pyrolysis of glucose-based carbohydrates at 500 °C. As shown, the model predictions closely match experimental data in terms of the individual yields and the overall trends as well, especially for the major products such as levoglucosan (pyranose), glycolaldehyde, 5-HMF, char, and CO_2. Even for the minor products furfural, levoglucosenone, and acetone, the model yields exhibit a striking match with the experimental data, and the trends across different carbohydrates are also captured well. Large errors for minor products (e.g., levoglucosenone shown in Figure 4c) from glucose pyrolysis might be due to the difficulties in controlling the sizes of glucose particles and accurately integrating the small peaks of those products in low yields on the gas chromatography. The yields of levoglucosan (furanose) and methyl glyoxal as a function of the size of the carbohydrates are also well-predicted with two outliers. Note that the yield of levoglucosan (pyranose) monotonically increased, and glycolaldehyde yields first went up then down slightly, while the yields of most of the other LMWPs and noncondensable gases decreased with an increase in chain length of the carbohydrates being pyrolyzed (Figures 3 and 4). Table 1 lists the predicted yields of other pyrolysis products that are not summarized in the figures. Mettler et al.[14,15] observed similar trends in the yields of many pyrolysis products

dx.doi.org/10.1021/ie502260q | Ind. Eng. Chem. Res. 2014, 53, 13290−13301

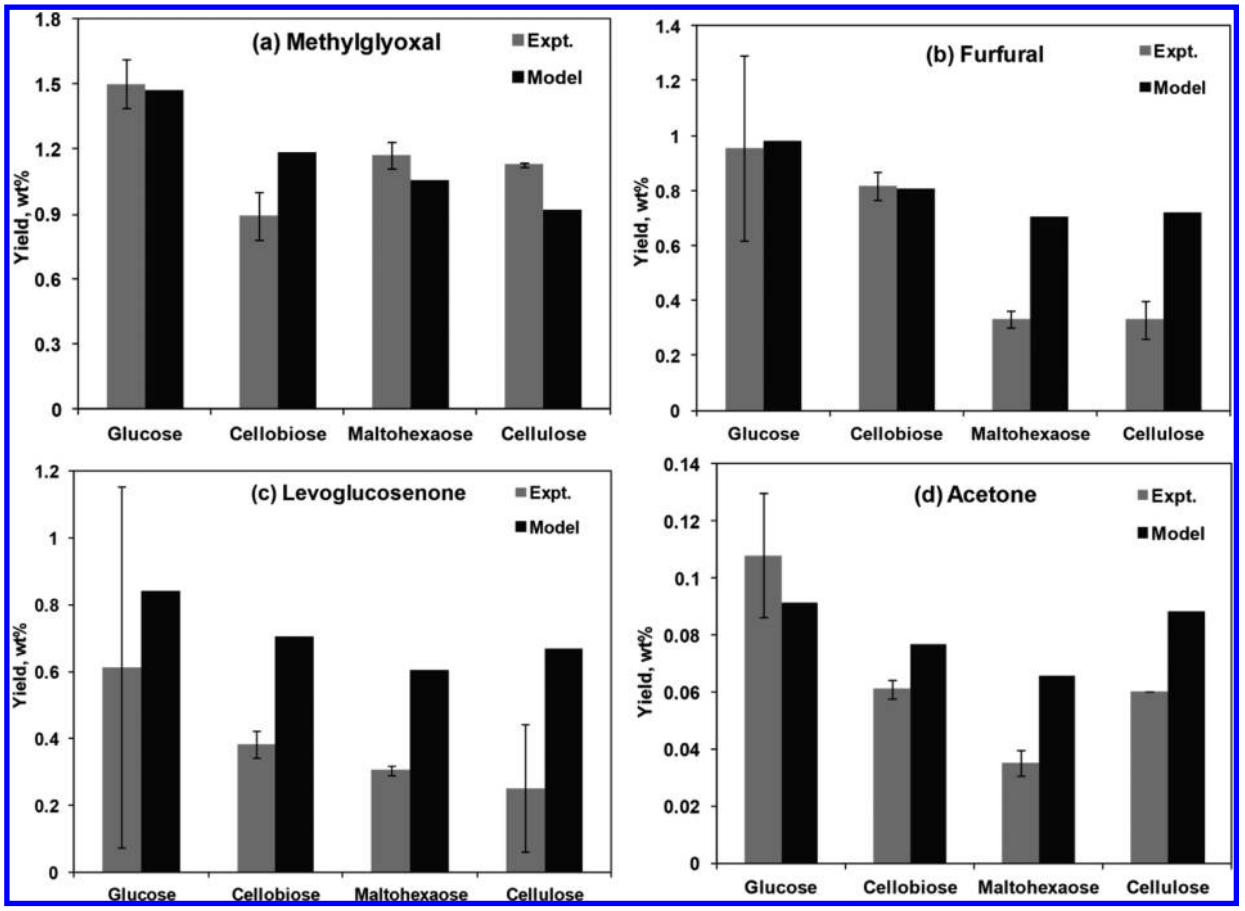

Figure 4. Comparisons between model predictions and experimental yields of minor products obtained from fast pyrolysis of glucose-based carbohydrates (glucose, cellobiose, maltohexaose, and cellulose) at 500 °C. The experimental error bars correspond to the standard deviation of triplicate fast pyrolysis runs for each case.

Table 1. Comparisons of Model Yields (in Weight Percent) of Various Pyrolysis Products with Experimental Data from Fast Pyrolysis of Glucose-Based Carbohydrates at 500 °C[a]

	glucose		cellobiose		maltohexaose		cellulose	
reactant	exptl	model	exptl	model	exptl	model	exptl	model
formic acid	—	0.35	—	0.28	—	0.24	—	0.14
formaldehyde	0.41	1.22	0.51	0.95	0.36	0.88	0.40	0.60
acetaldehyde	0.61	0.39	0.47	0.34	0.39	0.29	0.68	0.28
pyruvaldehyde[b]	—	1.30	—	0.95	—	0.82	—	0.24
glyceraldehyde[b]	—	0.10	—	0.06	—	0.05	—	0.03
glyoxal[c]	—	4.76	—	3.72	—	3.36	—	1.97
propenal	0.18	0.21	0.21	0.14	0.14	0.24	0.30	0.14
acetol	0.59	0.11	0.30	0.09	0.44	0.08	0.30	0.86
dihydroxyacetone	0.11	0.10	0.07	0.08	0.13	0.07	0.05	0.04
2-hydroxy-3-oxobutanal[d]	—	1.27	—	0.96	—	0.85	—	0.38
cyclic hydroxyl lactone	0.77	0.80	1.58	0.74	0.85	0.62	0.36	0.66
MW = 102[e]	0.12	0.87	0.12	0.63	0.03	0.54	0.08	0.15
furan methanol	0.09	0.10	0.05	0.08	0.22	0.07	0.07	0.08
anhydro/dehydrated sugars[e]	0.45	1.59	1.93	2.26	2.47	2.96	6.62	5.21
H_2	—	0.80	—	0.67	—	0.60	—	0.48
CO	1.2	1.65	1.11	1.40	1.23	1.18	1.84	1.10
H_2O	18.9	21.55	14.88	14.13	12.85	11.90	6.86	8.71

[a]All the experimental data are from the first part of this study (DOI 10.1021/ie502259w). The "—" symbol indicates products that were observed but not quantified in our experiments. [b]Products were identified in the isotopic labeling studies of Paine et al.[18] [c]Products were identified in the thin-film pyrolysis experiments of Mettler et al.[15] [d]Products were identified in pyrolysis experiments of Pattiya et al.[19] and Hodgson et al.[20] [e]The exact identity is unknown.

dx.doi.org/10.1021/ie502260q | Ind. Eng. Chem. Res. 2014, 53, 13290−13301

from cellulose through shorter chain oligomers to glucose monomer in thin-film pyrolysis experiments. As shown in Table 1, the model is able to predict the formation of other compounds such as formaldehyde, acetaldehyde, propenal, acetol, dihydroxyacetone, cyclic hydroxyl lactone, CO, and H_2O. Moreover, our experiments indicated the formation of pyrolysis products like formic acid, pyruvaldehyde, glyceraldehyde, glyoxal, 2-hydroxy-3-oxobutanal, and H_2 from fast pyrolysis of glucose-based carbohydrates, but were not able to quantify their yields, which the model can predict according to the pyrolysis mechanisms in this work. In addition to these products, the model also predicts the formation of products that were unidentified in the experiments, like anhydrosugars or compounds with molecular weight of 102 g·mol^{-1}.

Overall, the very good agreement of our model yields with experimental data for fast pyrolysis of glucose-based carbohydrates indicates that the mechanistic model built on the cellulose decomposition reaction mechanism and glucose as an intermediate for the formation of a range of LMW species is robust and extendable as well. Therefore, the present work is able to provide a better fundamental understanding of fast pyrolysis. As an example, the formation of levoglucosenone is apt. The existing mechanisms proposed in the literature to explain the formation of levoglucosenone from fast pyrolysis mostly involved levoglucosan as the intermediate. Lin et al.[16] proposed that levoglucosan can undergo dehydration and isomerization to form levoglucosenone and other anhydrosugars. Assary and Curtiss[17] reported dehydration pathways for the formation of levoglucosenone from levoglucosan. In contrast, our fast pyrolysis experiments using a micopyrolyzer-based system confirmed that levoglucosan was very volatile and would immediately undergo vaporization once it was formed, and no degradation occurred to levoglucosan formed during fast pyrolysis of neat glucose-based carbohydrates or levoglucosan as a reactant. In addition, our experimental work reported a decreasing trend (shown in Figure 4c) in the yield of levoglucosenone as a function of chain length of the reactant instead of an increasing trend, which would be expected if levoglucosenone is directly formed from levoglucosan because levoglucosan is produced in elevated yield from fast pyrolysis of carbohydrates with increasing chain length (shown in Figure 3a). Furthermore, our model, in which no secondary decomposition of levoglucosan is included, gives excellent agreement with experimental yields for levoglucosan from fast pyrolysis of glucose-based carbohydrates (Figure 3a) over a wide range of temperatures (Figure 1a) as well as striking agreement for a range of LMWPs including levoglucosenone (Figures 1–4). This is in sharp contrast to the existing mechanistic schemes in which secondary decomposition of levoglucosan is required to explain the formation of other LMWPs during fast pyrolysis.

3.3. Time Evolution of Pyrolysis Products and Reaction Time Scale of Fast Pyrolysis. Another advantage of the mechanistic model is that it is able to provide information and insights at the molecular level, which a lumped model can not provide and are difficult to obtain through experimental methods. For instance, besides predicting the final yields of the pyrolysis products, the model can also track the evolution of the product distribution of cellulosic chains and LMWPs during the entire duration of fast pyrolysis. As shown in Figure 5, the decomposition of cellulosic chains was completed within 1.5 s. At the initial stage of fast pyrolysis, 0.1–100 ms, the concentration of chains with a LVG-end on one end increases rapidly and reaches a maximum of 93 mol %. Simultaneously, the concentration of chains with a NR-end on one end was reduced to less than 6 mol % of all the species in the reaction system. After 100 ms, chains with a NR-end on one end and a LVG-end on the other end rapidly break down and few remain after 1.5 s. It is also clearly shown that the concentration of chains with dehydrated mid-groups and the resulting chains with an anhydroglucopyranose-end on one end increased sharply to a maximum at about 0.6–0.8 s and then dropped quickly.

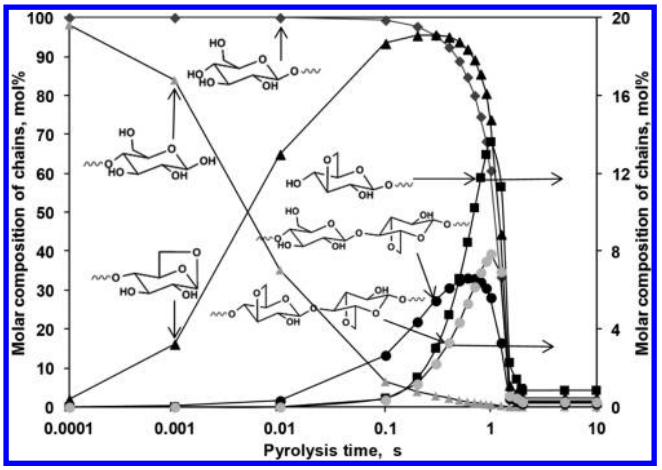

Figure 5. Time evolution of molar composition of cellulosic chains with end-groups and mid-groups during fast pyrolysis of cellulose at 500 °C.

A better understanding of the decomposition and evolution of cellulosic chains can be gained by performing net rate analysis. As shown in Figure 6, from 0.1 to 100 ms, the rate of initiation has a value of about 1.8 mol·L^{-1}· s^{-1}, much higher than those of depropagation and end-chain initiation as well as the thermohydrolysis reaction. The dominant role of initiation in decomposing cellulose at the initial pyrolysis stage leads to the rapid formation of numerous shorter chains with a NR-end on one end and a LVG-end on the other end (Figure 5). This is also consistent with the sharp decrease in DP of cellulose from 836 to about 45 within 100 ms and a slow decrease thereafter, as shown in Figure 7. From 100 ms to 1 s, the rates of

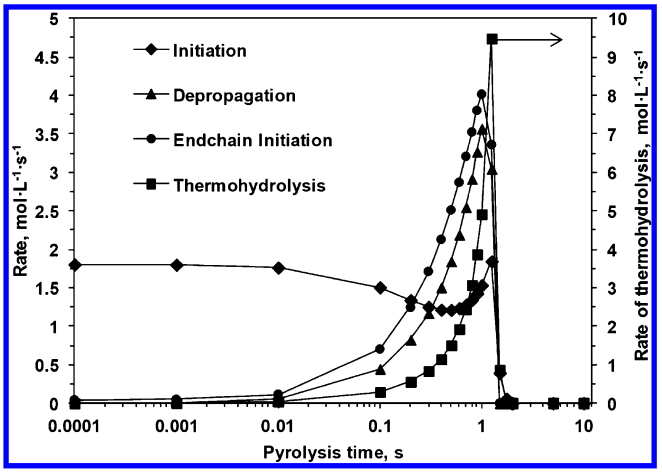

Figure 6. Variation of net rates of initiation, depropagation, end-chain initiation, and thermohydrolysis during fast pyrolysis of cellulose at 500 °C.

dx.doi.org/10.1021/ie502260q | Ind. Eng. Chem. Res. 2014, 53, 13290–13301

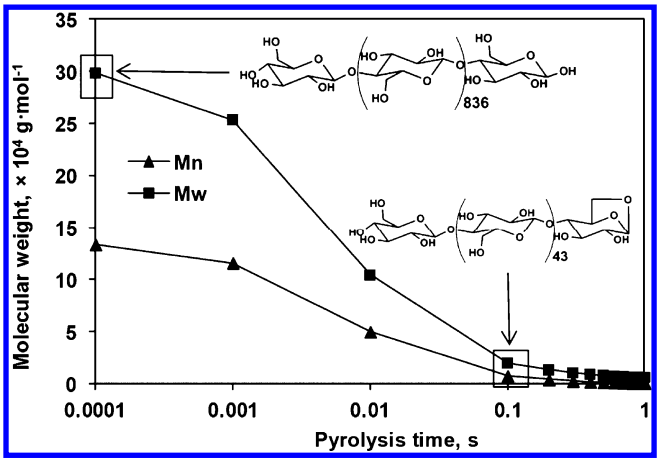

Figure 7. Time evolution of number-average (M_n) and weight-average (M_w) molecular weights of cellulose during fast pyrolysis at 500 °C.

depropagation and end-chain initiation drastically increase and reach their maximum values of 3.57 mol·L^{-1}·s^{-1} and 4.02 mol·L^{-1}· s^{-1}, respectively. Such high rates of end-chain initiation and depropagation result in rapid formation of levoglucosan (Figure 9) from opposite ends of the cellulosic chains. 1,2-Dehydration and retro-Diels−Alder also can happen to a NR-end to form chains with other end-groups, which will eventually be converted to LVG-end chains via end-chain initiation. However, midchain dehydration forms chains with a dehydrated mid-group, which leads to the formation of chains with an anhydroglucopyranose-end on one end. Moreover, the yield of water, a product of dehydration, increases as pyrolysis proceeds (Figure 9). Thermohydrolysis, assisted by the involvement of water to produce glucose and 3,6-anhydroglucopyranose, increases sharply, and its rate reaches a maximum of 9.48 mol·L^{-1}·s^{-1} from 100 ms to 1.25 s. As a result, yields of glucose (Figure 8) and glycolaldehyde (Figure 9) derived from

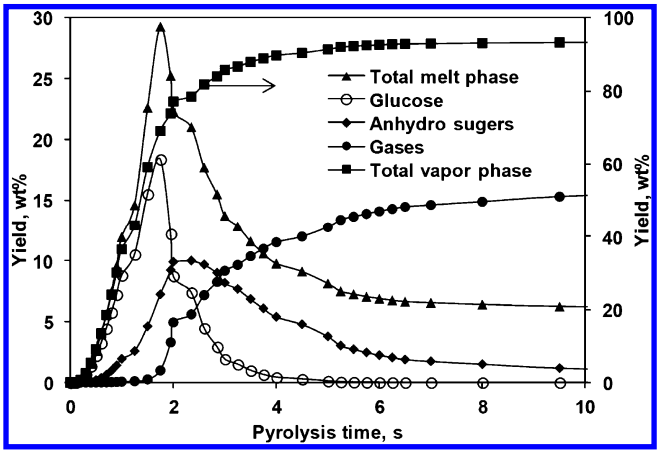

Figure 8. Time evolution of various lumped fractions including melt phase, vapor phase, gases, anhydro/dehydrated sugars, and glucose intermediate during fast pyrolysis of cellulose at 500 °C.

3,6-anhydroglucopyranose undergo large increases over the corresponding period of time. Glucose formed from cellulose decomposition is then converted to various anhydrosugars and LMWPs according to reaction mechanisms in Schemes S3 and S4 in the Supporting Information. Therefore, as shown in Figure 8, the concentration of melt phase species that includes glucose, various dehydrated products of glucose, C5 intermediates, and char, reaches a maximum at ∼1.75 s. Afterward, the yields of glucose and other melt phase species both sharply decrease. Subsequently, the vapor phase species are produced with a rising yield, and anhydrosugars reach a yield maximum at 2.4 s. As a result of anhydrosugars being converted, yields of char (Figure 9) and gaseous species including CO_2, CO, H_2O, and H_2 (Figures 8 and 9), which are mainly formed from anhydrosugars via char formation as depicted in Scheme S5 in the Supporting Information, go up quickly after 2 s. At the same time, melt phase species finally reach a constant yield after 5 s, corresponding to char that is the only species in the melt phase. The final yields of char and gaseous species agree well with the experimental yields, supporting the conclusion that the simplified char formation reactions are representative of the actual condensation and repolymerization reactions that might occur during char formation.

The evolution dynamics of individual products during fast pyrolysis are depicted in Figure 9. It can be observed that levoglucosan was the first pyrolysis product that reached a constant yield within 1.75 s, indicating that levoglucosan was primarily formed from chain decomposition and also that the formation of levoglucosan during fast pyrolysis was facile. Besides levoglucosan, glycolaldehyde and water vapor also showed a sharp increase in yield before 2 s because they also can be directly formed from the decomposition of cellulose chains instead of from intermediate glucose only. Intermediate glucose was formed in large measure via thermohydrolysis and then converted to its major products like levoglucosan (pyranose), levoglucosan (furanose), glycolaldehyde, 5-HMF, char, and CO_2, leading to the rapid increase in yields of the corresponding products within 1.5 to 2.5 s. The decrease in yield of 5-HMF is caused by the char formation emanating from 5-HMF, which is a highly dehydrated product and likely to form char during exposure to high temperatures. The other LMWPs that originate from the melt phase species undergo a gradual increase in yield and then attain a constant concentration within 4−5 s. Therefore, the time taken for complete conversion of cellulose during fast pyrolysis at 500 °C corresponds to 4−5 s. The time evolution of LMWPs is even clearer from Figure S1 in the Supporting Information, which plots the evolution profiles of various products from the fast pyrolysis of glucose.

3.4. Effect of Initial Chain Length of Glucose-Based Carbohydrates. The effects of initial chain length of glucose-based carbohydrates on the overall weight loss kinetics and the evolution of individual products were investigated. Note that, for modeling fast pyrolysis of cellulose with varying initial DP, the polydispersity of different cellulose samples was set to 2.0. Figure 10 shows the evolution of the overall weight loss of the initial samples during fast pyrolysis. The overall weight loss profiles correspond to the evolution of the yield of total melt phase species, including unconverted cellulosic polymer chains, C5/C6 sugars, dehydrated sugars, and char. It can be seen that the total yield of melt phase species reached a constant value within 4 s, corresponding to complete thermoconversion of all the carbohydrates and their derivative intermediates, while no difference was observed for the mass loss profiles of cellulose with different initial DP. Subtle differences among glucose, cellobiose/maltohexaose, and cellulose were observed. Note that the existing lumped kinetic models that have been developed for fast pyrolysis were based on experimental data

dx.doi.org/10.1021/ie502260q | Ind. Eng. Chem. Res. 2014, 53, 13290−13301

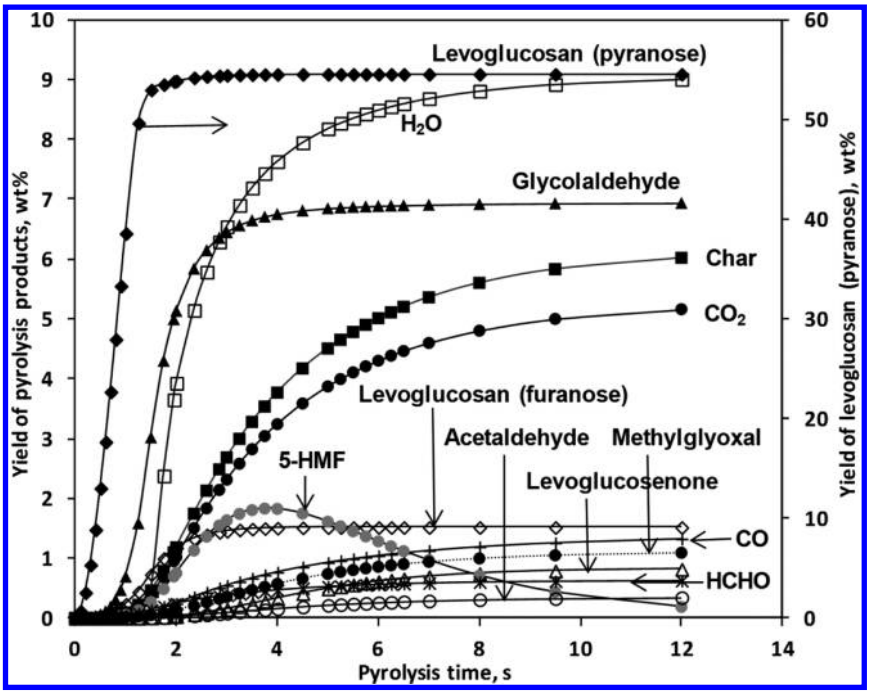

Figure 9. Time evolution of various LMWPs during fast pyrolysis of cellulose at 500 °C.

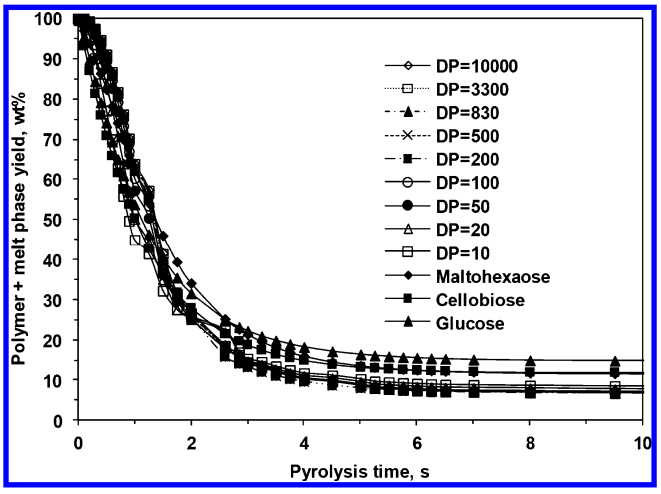

Figure 10. Time evolution of overall weight loss predicted by the model of cellulose with different initial DP, maltohexaose, cellobiose, and glucose during fast pyrolysis at 500 °C.

obtained with thermogravimetric analyzers, which measure the overall weight loss of samples.

Figure 11 depicts the final yields of major products such as levoglucosan (pyranose), char, CO_2, 5-HMF, glycolaldehyde, and levoglucosan (furanose) from fast pyrolysis of cellulose with different initial DP, maltohexaose, cellobiose, and glucose at 500 °C. It was shown that the yields of these products remained unchanged for celluloses with an initial DP greater than 500, slightly changed as DP was reduced from 500 to 50, and changed significantly as DP was further reduced. This trend is much clearer in the time evolution of levoglucosan from fast pyrolysis of glucose-based carbohydrates (Figure S2 in the Supporting Information). Modeling results indicated that the chain length of cellulose has a negligible effect when it is greater than 500, while the kinetics of individual pathways that lead to the formation of LMWPs are influenced by degradation of the chains with a length less than 50. Despite the significant changes in the yields of individual pyrolysis products, the reduction in initial chain length of the carbohydrates shows a negligible effect on altering the kinetics of their overall mass loss during fast pyrolysis. The mechanistic model is able to provide a much clearer picture for the molecular speciation of the pyrolysis products than lumped models while still reporting overall mass loss kinetics.

3.5. Analysis of the Contributions of Different Pathways for the Formation of Levoglucosan and Glycolaldehyde. Another advantage of mechanistic modeling lies in the analysis of the contributions of different pathways leading to the formation of key products and its ability to gain insight into the competitive nature of complex reaction systems. Levoglucosan is the dominant product of fast pyrolysis of cellulose. As described in Schemes S1−S3 in the Supporting Information, there are three main pathways to form levoglucosan from cellulose: (1) end-chain initiation of cellulose with a NR-end; (2) depropagation of LVG-end chains which can be formed by initiation, dehydration, and end-chain initiation; and (3) one-step dehydration of a glucose intermediate. To evaluate the contributions of different pathways that lead to the formation of levoglucosan from fast pyrolysis, the variation of the final yields of levoglucosan through these three pathways is plotted in Figure 12a as a function of different temperatures for fast pyrolysis of cellulose and in Figure 12b for different pyrolysis substrates. As shown in Figure 12a, as the pyrolysis temperature rose from 400 to 600 °C, levoglucosan directly formed from decomposition of the cellulosic chains through end-chain initiation decreased from 35.7 to 21.8 wt %, and through depropagation decreased from 26.3 to 18.8 wt %. However, the two pathways still account for the majority of the levoglucosan in the final yield, and the pathway of glucose dehydration to levoglucosan contributes only a small proportion, though its yield increases from 2.96 to 3.41 wt %. Dehydration, especially midchain dehydration, was the main cause for the decreasing yield and contribution of

dx.doi.org/10.1021/ie502260q | Ind. Eng. Chem. Res. 2014, 53, 13290−13301

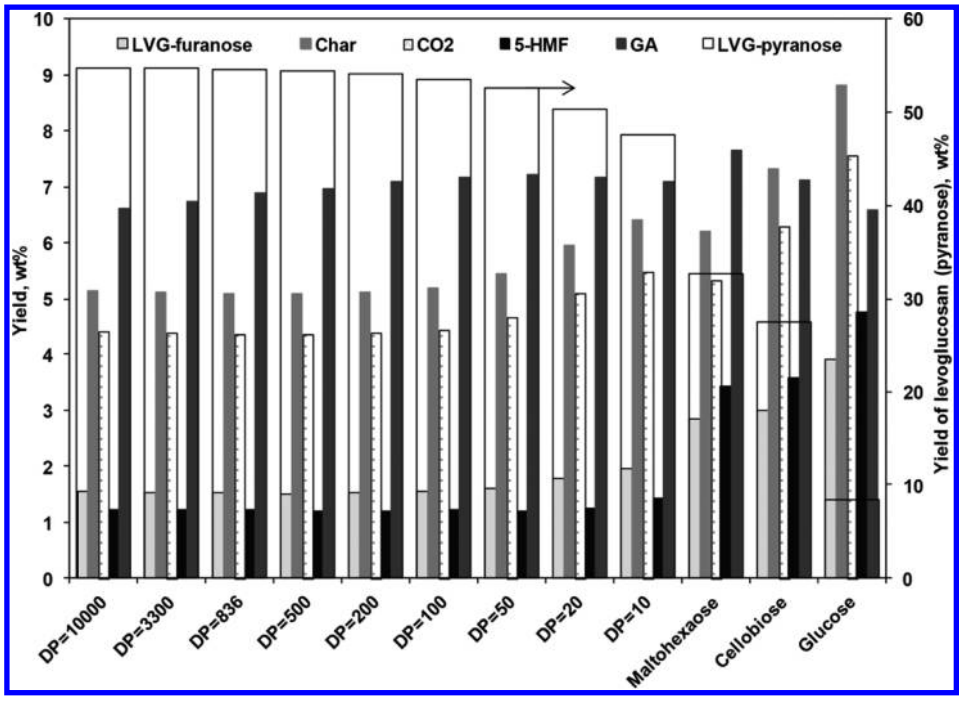

Figure 11. Final yields of major products from fast pyrolysis of cellulose with different initial DP, maltohexaose, cellobiose, and glucose at 500 °C.

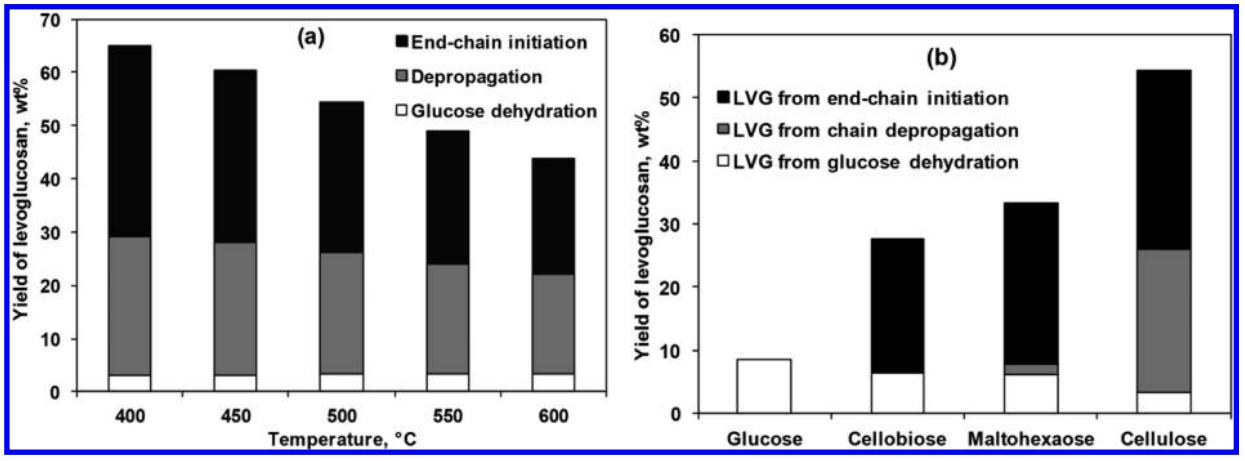

Figure 12. Contributions of different pathways to the formation of levoglucosan (LVG) derived from fast pyrolysis of (a) cellulose at temperatures ranging from 400 to 600 °C and (b) glucose-based carbohydrates (glucose, cellobiose, maltohexaose, and cellulose) at 500 °C, obtained from the mechanistic model presented in this work.

levoglucosan directly formed from the chains. Because of its higher activation energy of 60 kcal·mol^{-1}, midchain dehydration is favored at high pyrolysis temperatures and thus leads to faster formation of water, which in turn promotes the thermohydrolysis to form glucose and 3,6-anhydroglucopyranose in the initial pyrolysis stage as temperature increases. As a result, the contributions of end-chain initiation and depropagation decrease and that of glucose dehydration increases in the formation of levoglucosan. Furthermore, because LVG-end chains can be formed from the chains with dehydrated midgroups via midchain glycosidic bond cleavage, a relatively slower decline is observed for the contribution of the depropagation pathway as compared with that of the end-chain initiation pathway varying with elevated temperature. However, as shown in Figure 12b, a sharp decrease in yield of levoglucosan formed via depropagation was observed from cellulose (DP = 836) to maltohexaose (DP = 6), while the yields of levoglucosan formed via end-chain initiation only slightly decreased. The contribution of end-chain initiation to the final yield of levoglucosan increased from cellulose to cellobiose (DP = 2). This is consistent with the decomposition mechanism of the chains, in which end-chain initiation occurs independently of midchain initiation, while depropagation requires the generation of LVG-end chains through midchain initiation, the rate of which decreases with the reduction in chain length. The yield from the glucose dehydration pathway and its contribution to the final yield of levoglucosan increased with the reduction in the chain length of the carbohydrates being pyrolyzed.

As described in Schemes S1−S4 in the Supporting Information, the pathways leading to the formation of glycolaldehyde via a final elementary step of retro-aldol (reactions 18, 44, 48, and 70), retro-Diels−Alder reactions (reactions VII, XII, ix, 5, 9, and 61), or enol-keto

dx.doi.org/10.1021/ie502260q | Ind. Eng. Chem. Res. 2014, 53, 13290−13301

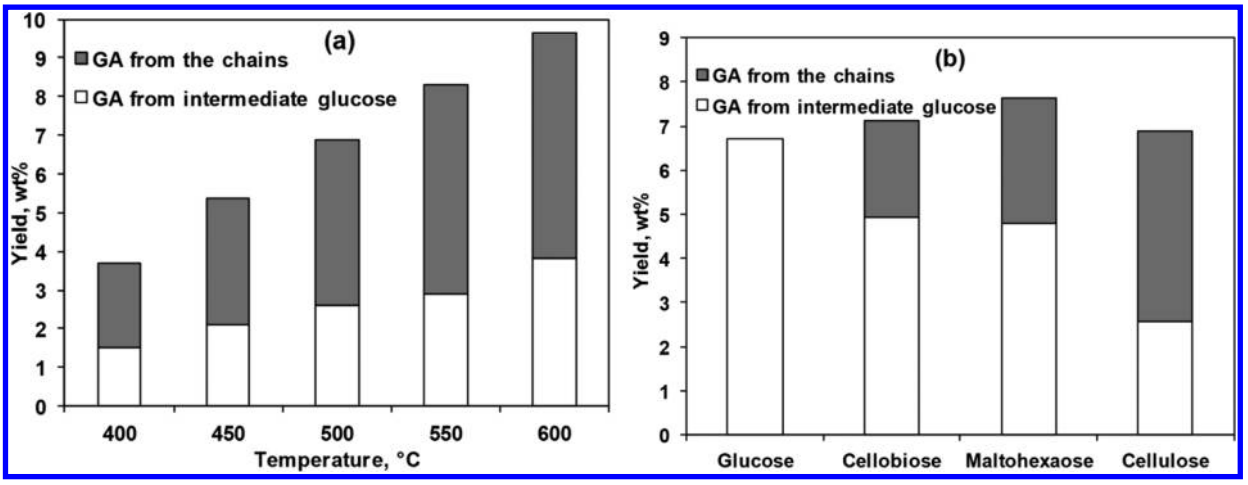

Figure 13. Contributions of pathways to the formation of glycolaldehyde derived from fast pyrolysis of (a) cellulose at temperatures ranging from 400 to 600 °C and (b) glucose-based carbohydrates (glucose, cellobiose, maltohexaose, and cellulose) at 500 °C, obtained from the mechanistic model presented in this work.

tautomerization (reaction 49) can be classified into two routes. One route is glycolaldehyde directly formed through decomposition of the chains, including pathways through reactions VII, XII, and ix. The other is that the formation of glycolaldehyde requires the involvement of a glucose intermediate. As shown in Figure 13a, the yields of glycolaldehyde directly formed from the chains and from intermediate glucose both increase with rising pyrolysis temperatures. The reason for the variations is similar to that for the decreasing yields of levoglucosan with increasing temperatures; that is, higher temperatures favor dehydration, affording water at a faster rate. Subsequently, more glucose and 3,6-anhydroglucopyranose (intermediate for reaction ix) are produced via thermohydrolysis. Another feature is that the rate of glycolaldehyde formation from the chains increased faster than that from a glucose intermediate; thus, its contribution to the final yield of glycolaldehyde also increased. Glycolaldehyde can also be formed through end-chain initiation (reactions iii and vi) with a higher E_a of 56 kcal·mol^{-1}, which is favored at high pyrolysis temperatures compared to thermohydrolysis. The modeling results also suggest that the pathway through reaction ix and the pathway through reactions 44, 48, and 49 contribute most significantly to each route for glycolaldehyde production. Because the reaction probability and reaction rate of midchain dehydration and midchain glycosidic bond cleavage decreased with a reduction in chain length, both the yield of glycolaldehyde directly formed from the chains and its contribution to the total yield decreased from cellulose to glucose, as shown in Figure 13b. Increased formation of levoglucosan and glycolaldehyde from carbohydrates with increasing chain length led to decreased formation of intermediate glucose; thus, the yield of glycolaldehyde from glucose intermediates decreased with increasing chain length (Figure 13b). Therefore, a maximum yield of glycolaldehyde from maltohexaose pyrolysis was observed in experiments and captured by the model as shown in Figure 3c.

It is shown that competition exists between the formation of glycolaldehyde and glucose as well as levoglucosan from the decomposition of cellulosic chains during fast pyrolysis. Besides levoglucosan and glycolaldehyde, the mechanistic model also depicts the formation of many other pyrolysis products and provides a better understanding of the nature of competing reactions in fast pyrolysis in terms of the final yields and underlying chemistry. This then opens up the possibility of actively controlling the yield and selectivity of particular pyrolysis products, such as the valuable platform chemical 5-HMF or the pharmaceutical intermediate levoglucosenone, by tweaking specific reactions through catalysis and optimization of the reaction conditions.

4. CONCLUSIONS

In this work, validation of the mechanistic model was performed by comparing modeling results, obtained by utilizing the same set of kinetic parameters that were based on experimental measures and quantum chemical calculations from the literature, with experimental yields from fast pyrolysis at different temperatures and for different carbohydrates. Very good agreement over a wide range of reaction conditions and substrates demonstrated that the mechanistic model is robust and extendable. The model was able to predict the yields and trends of the major products, such as levoglucosan, 5-HMF, glycolaldehyde, char, H_2O, CO_2, CO, and methyl glyoxal, and minor products like levoglucosenone, furfural, acetone, dihydroxyacetone, propenal, as well as pyrolysis products that were not quantified or identified in experiments such as pyruvaldehyde, glyceraldehyde, glyoxal, and 2-hydroxy-3-oxobutanal.

In addition to predicting the final yields of pyrolysis products, the model was also able to provide the time evolution of the product distribution and determine the reaction time scale of fast pyrolysis. The formation of levoglucosan and the thermoconversion of cellulose to various LMWPs in fast pyrolysis of cellulose at 500 °C were completed within 1.75 s and 4−5 s, respectively. Both experimental and modeling results indicate that levoglucosan formed from fast pyrolysis of neat carbohydrates does not undergo subsequent degradation.

Analysis of net reaction rates and contributions of pathways provides a better understanding of the nature of competitive reactions leading to pyrolysis products. Levoglucosan formed via end-chain initiation and depropagation contributes more than that from dehydration of glucose to its final yield and shows a diminishing role with rising temperature and also with a reduction in chain length of the reactant. The yield of glycolaldehyde directly formed from the decomposition of

dx.doi.org/10.1021/ie502260q | Ind. Eng. Chem. Res. 2014, 53, 13290−13301

cellulosic chains and its contribution to its final yield increases with pyrolysis temperature and decreases with a reduction in chain length of the initial reactant.

The mechanistic model for fast pyrolysis of neat glucose-based carbohydrates provides a basis for studying catalytic interventions in cellulose pyrolysis, including the action of naturally occurring inorganic salts. Extending the model to quantify the effects of inorganic salts on fast pyrolysis at the mechanistic level is underway. A similar modeling methodology can be applied for unraveling the decomposition kinetics and mechanism of fast pyrolysis of hemicelluloses and lignin, allowing for advances toward a mechanistic understanding of fast pyrolysis of biomass.

■ ASSOCIATED CONTENT

Supporting Information

Yields (in weight percent) of the chemical species arising from fast pyrolysis of neat cellulose at 400−600 °C (Table S1) and corresponding standard deviation for triplicate pyrolysis runs (Table S2); yields (in weight percent) of the chemical species arising from fast pyrolysis of neat glucose, cellobiose, and maltohexaose at 500 °C (Table S3) and corresponding standard deviation for triplicate pyrolysis runs (Table S4); Arrhenius rate parameters of different reaction types used in the mechanistic model of fast pyrolysis of glucose-based carbohydrates (Table S5); time evolution of various LMWPs during fast pyrolysis of glucose at 500 °C (Figure S1); time evolution of levoglucosan from fast pyrolysis of cellulose with different initial DP, maltohexaose, cellobiose, and glucose at 500 °C (Figure S2); and reaction mechanism of fast pyrolysis of neat glucose-based carbohydrates (Schemes S1−S5). This material is available free of charge via the Internet at http://pubs.acs.org.

■ AUTHOR INFORMATION

Corresponding Author

*E-mail: broadbelt@northwestern.edu. Fax: +1-847-491-3728. Tel: +1-847-491-5351.

Notes

The authors declare no competing financial interest.

■ ACKNOWLEDGMENTS

The authors are grateful for financial support provided by the Department of Energy (DOE) Office of Energy Efficiency and Renewable Energy (EERE) through the Office of Biomass Program, Grant DEEE0003044. The authors thank Dr. R. Vinu, Heather B. Mayes, and Abraham J. Yanez-McKay for fruitful discussions and useful suggestions.

■ REFERENCES

(1) Vispute, T. P.; Zhang, H.; Sanna, A.; Xiao, R.; Huber, G. W. Renewable Chemical Commodity Feedstocks from Integrated Catalytic Processing of Pyrolysis Oils. *Science* **2010**, *330*, 1222−1227.

(2) Regalbuto, J. R. Cellulosic Biofuels—Got Gasoline? *Science* **2009**, *325*, 822−824.

(3) Vinu, R.; Broadbelt, L. J. A Mechanistic Model of Fast Pyrolysis of Glucose-Based Carbohydrates to Predict Bio-oil Composition. *Energy Environ. Sci.* **2012**, *5*, 9808−9826.

(4) Vinu, R.; Broadbelt, L. J. Unraveling Reaction Pathways and Specifying Reaction Kinetics for Complex Systems. *Annu. Rev. Chem. Biomol. Eng.* **2012**, *3*, 29−54.

(5) Lédé, J. Cellulose Pyrolysis Kinetics: An Historical Review on the Existence and Role of Intermediate Active Cellulose. *J. Anal. Appl. Pyrolysis* **2012**, *94*, 17−32.

(6) Kodera, Y.; McCoy, B. J. Distribution Kinetics of Radical Mechanisms: Reversible Polymer Decomposition. *AIChE J.* **1997**, *43*, 3205−3214.

(7) Kruse, T. M.; Woo, O. S.; Wong, H. W.; Khan, S. S.; Broadbelt, L. J. Mechanistic Modeling of Polymer Degradation: A Comprehensive Study of Polystyrene. *Macromolecules* **2002**, *35*, 7830−7844.

(8) Wang, M.; Smith, J. M.; McCoy, B. J. Continuous Kinetics for Thermal Degradation of Polymer in Solution. *AIChE J.* **1995**, *41*, 1521−1533.

(9) McCoy, B. J. Continuous-mixture Kinetics and Equilibrium for Reversible Oligomerization Reactions. *AIChE J.* **1993**, *39*, 1827−1833.

(10) McCoy, B. J.; Madras, G. Evolution to Similarity Solutions for Fragmentation and Aggregation. *J. Colloid Interface Sci.* **1998**, *201*, 200−209.

(11) Stewart, W. E.; Caracotsios, M.; Sorenson, J. P. *Appendix A. DDASAC Software Package Documentation*. Department of Chemical Engineering, University of Wisconsin: Madison, WI, 1994.

(12) Mayes, H. B.; Nolte, M. W.; Beckham, G. T.; Shanks, B. H.; Broadbelt, L. J. The Alpha-Bet(a) of Glucose Pyrolysis: Computational and Experimental Investigations of 5-Hydroxymethylfurfural and Levoglucosan Formation Reveal Implications for Cellulose Pyrolysis. *ACS Sustainable Chem. Eng.* **2014**, *2*, 1461−1473.

(13) Paulsen, A. D.; Mettler, M. S.; Dauenhauer, P. J. The Role of Sample Dimension and Temperature in Cellulose Pyrolysis. *Energy Fuels* **2013**, *27*, 2126−2134.

(14) Mettler, M. S.; Paulsen, A. D.; Vlachos, D. G.; Dauenhauer, P. J. The Chain Length Effect in Pyrolysis: Bridging the Gap Between Glucose and Cellulose. *Green Chem.* **2012**, *14*, 1284−1288.

(15) Mettler, M. S.; Mushrif, S. H.; Paulsen, A. D.; Javadekar, A. D.; Vlachos, D. G.; Dauenhauer, P. J. Revealing Pyrolysis Chemistry for Biofuels Production: Conversion of Cellulose to Furans and Small Oxygenates. *Energy Environ. Sci.* **2012**, *5*, 5414−5424.

(16) Lin, Y. C.; Cho, J.; Tompsett, G. A.; Westmoreland, P. R.; Huber, G. W. Kinetics and Mechanism of Cellulose Pyrolysis. *J. Phys. Chem. C* **2009**, *113*, 20097−20107.

(17) Assary, R. S.; Curtiss, L. A. Thermochemistry and Reaction Barriers for the Formation of Levoglucosenone from Cellobiose. *ChemCatChem.* **2012**, *4*, 200−205.

(18) Paine, J. B., III; Pithawalla, Y. B.; Naworal, J. D. Carbohydrate Pyrolysis Mechanisms from Isotopic Labeling: Part 3. The Pyrolysis of D-Glucose: Formation of C3 and C4 Carbonyl Compounds and a Cyclopentenedione Isomer by Electrocyclic Fragmentation Mechanisms. *J. Anal. Appl. Pyrolysis* **2008**, *82*, 42−69.

(19) Pattiya, A.; Titiloye, J. O.; Bridgwater, A. V. Fast Pyrolysis of Cassava Rhizome in the Presence of Catalysts. *J. Anal. Appl. Pyrolysis* **2008**, *81*, 72−79.

(20) Hodgson, E. M.; Nowakowski, D. J.; Shield, I.; Riche, A.; Bridgwater, A. V.; Clifton-Brown, J. C.; Donnison, I. S. Variation in Miscanthus Chemical Composition and Implications for Conversion by Pyrolysis and Thermo-chemical Bio-refining for Fuels and Chemicals. *Bioresour. Technol.* **2011**, *102*, 3411−3418.